Available online at www.sciencedirect.com
ScienceDirect
Tetrahedron 63 (2007) 9774–9783
Tetrahedron

Molecular engineering of hybrid π-conjugated oligomers combining 3,4-ethylenedioxythiophene (EDOT) and thiophene-*S*,*S*-dioxide units

Manuela Melucci,[a,*] Pierre Frère,[b,*] Magali Allain,[b] Eric Levillain,[b] Giovanna Barbarella[a] and Jean Roncali[b]

[a]*Istituto per la Sintesi Organica e la Fotoreattività (ISOF), Consiglio Nazionale Ricerche, Via Gobetti 101, 40129 Bologna, Italy*
[b]*Laboratoire Chimie, Ingénierie Moléculaire et Matériaux d'Angers (CIMMA), UMR CNRS 6200, Université d'Angers, Département de Chimie, 2 Boulevard Lavoisier, 49045 Angers, France*

Received 8 June 2007; accepted 4 July 2007
Available online 10 July 2007

Abstract—A series of π-conjugated oligomers based on various combinations of thiophene, 3,4-ethylenedioxythiophene (EDOT) and thiophene-*S*,*S*-dioxide units have been synthesized. Theoretical calculations, optical and electrochemical data show that the relative positions of EDOT and *S*,*S*-dioxide units in the conjugated system exert strong influence on its electronic properties. The insertion of EDOT units inside the conjugated chain with the *S*,*S*-dioxide units located at the lateral positions leads to a planar conjugated system presenting moderate band gap. In contrast, substituted *S*,*S*-dioxide units located within the backbone produce a torsion of the conjugated chain. However, the twist angle is significantly reduced when the EDOT and *S*,*S*-dioxide moieties are separated by unsubstituted thiophene cycles. Introduction of *S*,*S*-dioxide unit in the median position of the chain has a stronger effect on the lowering of the LUMO level while insertion of EDOT units at the lateral positions limits the decrease of the HOMO level. Consequently, the corresponding oligomers present the smallest electrochemical gap while electrooxidation leads directly to the dication state through a bi-electronic process.

1. Introduction

The control of the electronic properties of thiophene-based conjugated polymers and oligomers remains at the forefront of research on linearly π-conjugated systems.[1–3] Based on their well-defined chemical structure, conjugated oligomers have been extensively investigated for the analysis of structure–properties relationships and as models of parent polydisperse polymers.[4] In parallel, conjugated oligomers have been widely used as active materials for the fabrication of optoelectronic devices[5] such as field-effect transistors,[6–10] light-emitting diodes[11–13] and photovoltaic cells.[14–20] Extensive studies aiming at the modification of the oligothiophene backbone have been carried out in order to control the energy levels of the HOMO and LUMO frontier orbitals and thus crucial electronic properties such as ionization potential, electron affinity, and absorption and emission properties. Synthetic approaches involving various structural factors, such as chain extension, planarity, insertion of electron-donor or electron-acceptor groups, reduction of the overall aromaticity of the conjugated system, have been developed in order to control the energy gap of oligothiophenes.[3]

In this context, 3,4-ethylenedioxythiophene (EDOT) has progressively emerged as an important versatile building block for the molecular engineering of functional π-conjugated systems with tailored electronic properties.[21,22] In addition to the strong electron-donor effect of the ethylenedioxy group, which can serve to raise the HOMO level, it has been shown that the insertion of an EDOT unit in a conjugated chain gives rise to intramolecular non-covalent sulfur–oxygen interactions, which result in the self-rigidification of the conjugated chain. Oligo-EDOT[23–25] and hybrid EDOT-thiophene oligomers[26,27] have been synthesized and the analysis of their structure and electronic properties has shown that a judicious use of EDOT as building block allows a fine tuning of the electronic properties of π-conjugated systems.

On the other hand, it has been demonstrated that incorporation of thiophene-*S*,*S*-dioxide units in the oligothiophene backbone[28–30] or the synthesis of all-*S*,*S*-dioxide oligothiophenes[31] also represents an efficient method for tuning the electronic properties of the corresponding conjugated system due to the combined effects of the decrease of the overall aromaticity and of the lowering of the LUMO level.

As a further step in our continuing interest in the control of the electronic properties of oligothiophenes, we describe here the synthesis and characterization of a new series of

* Corresponding authors. Tel.: +33 241735063; fax: +33 241735405; e-mail: pierre.frere@univ-angers.fr

0040–4020/$ - see front matter © 2007 Elsevier Ltd. All rights reserved.
doi:10.1016/j.tet.2007.07.006

hybrid oligomers based on various combinations of EDOT (E) and substituted thiophene-*S*,*S*-dioxide units (O) (Scheme 1). The structures and electronic properties of the various oligomers have been analyzed by X-ray diffraction, UV–vis spectroscopy, cyclic voltammetry and theoretical calculations and the results are discussed with regard to the influence of the number and relative positions of the O and E units on the electronic properties of the π-conjugated backbone.

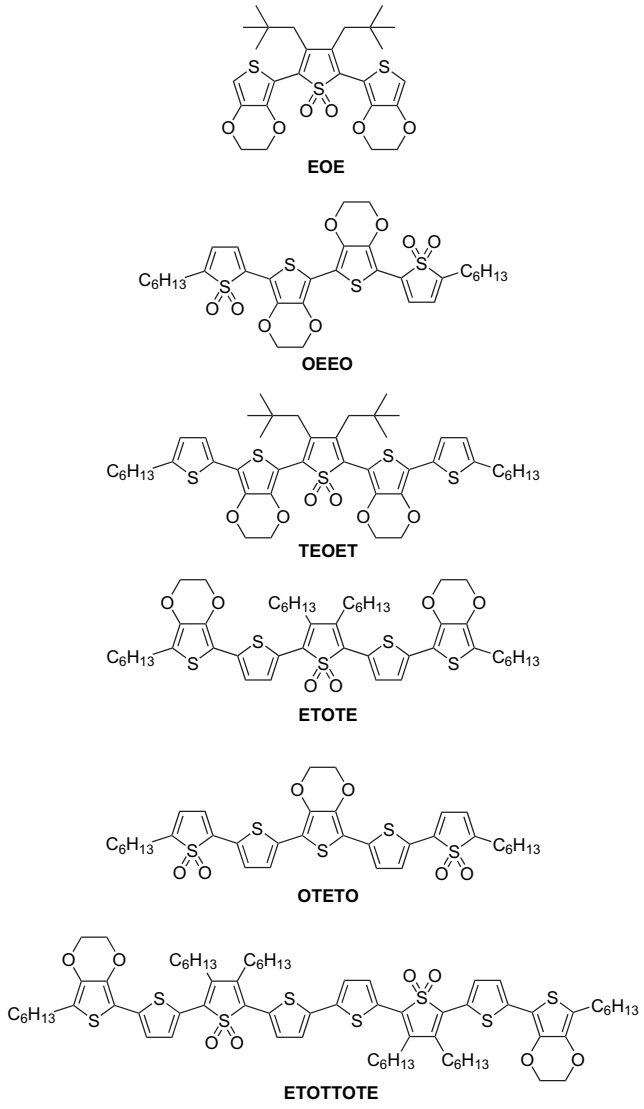

Scheme 1. Structures of the hybrid oligomers.

2. Results and discussions

2.1. Synthesis

The synthesis of the various oligomers is described in Scheme 2. All target compounds have been synthesized by Stille coupling reactions, the bromine atoms are always grafted on the building unit containing the sulfone moieties. Tetramer **OEEO** was obtained in 20% yield by a twofold Stille coupling between the bromo sulfone **1** and the distannyl derivative of bis-EDOT **2**. **EOE** was prepared in 75% yield by a twofold coupling between a slight excess of stannyl derivative of EDOT **4** and dibromosulfone **3**. The dibromo derivative **5** was obtained in 80% yield by treatment of **EOE** with 2 equiv of *N*-bromosuccinimide in chloroform. A second twofold Stille coupling between **5** and 2-hexyl-5-tributylstannyl-thiophene **6** afforded pentamer **TEOET** in 62% yield. Application of the *n*-BuLi/Bu_3SnCl sequence on terthiophene **7** gave the distannyl derivative **8**. Reaction of this latter compound with a slight excess of sulfone **1** gave the pentamer with two terminal hexylsulfone moieties **OTETO** in 10% yield whereas compound **9** corresponding to a single coupling reaction was isolated in 35% yield.

The synthesis of pentamer **ETOTE** involved first a coupling of 2,5-dibromo-3,4-dihexylthiophene sulfone **10** with 2-tributylstannylthiophene **11** to afford trimer **12** in 80% yield. This compound was then converted into the corresponding dibromo derivative **13** with NBS in $CHCl_3$/AcOH solution. A Stille coupling between **13** and the stannyl derivative of 2-hexyl-EDOT **14** gave the target compound in 54% yield together with octamer **ETOTTOTE** (10%) as a side product.

2.2. Crystallographic structures

The crystallographic structures of single crystals of **EOE** and **ETOTE** obtained by slow evaporation of chloroform/ethanol solutions have been analyzed by X-ray diffraction. These two structures reveal strong differences between the conformations of the two conjugated systems.

EOE co-crystallizes with a molecule of $CHCl_3$ in the monoclinic space group $P2_1/n$. As shown in Figure 1, the structure of **EOE** is not planar. The two neopentyl groups are located above and below the plane defined by the central ring moiety. The conformation of the molecule is characterized by important inter-ring torsions and the EDOT moieties form S–C–C–S dihedral angles of 46° and 51°, respectively, with the central *S*,*S*-dioxide unit. These twist angles are considerably higher than those found for trimer **12**[32] (28.5° and 11.6°, respectively). Both the neopentyl and ethylenedioxy groups contribute to the steric hindrance, which induces a severe torsion of the molecule and thus limits the effective conjugation length.

Examination of bond lengths of the two heterocycles reveals notable differences between thiophene and *S*,*S*-dioxide thiophene moieties. Thus for the central ring, the C05–S02, C08–S02 and C06–C07 bonds are lengthened while the C05–C06 and C07–C08 bonds are shortened. Such an effect corresponds to the loss of the aromatic character of the thienyl-*S*,*S*-dioxide moiety.

For **ETOTE**, the very small thickness of the obtained crystals together with the existence of strong disorder in the hexyl chains attached on the median and lateral rings did not allow to reach a high structural resolution. Nevertheless, the atomic positions of the conjugated systems can be clearly localized and they show that the backbone is quasi-planar (Fig. 2). The two lateral EDOT-thiophene blocks are fully planar and they form dihedral angles smaller than 5° with the central *S*,*S*-dioxide unit.

Comparison of these data with the structure of **EOE** shows that the insertion of unsubstituted thiophene rings between

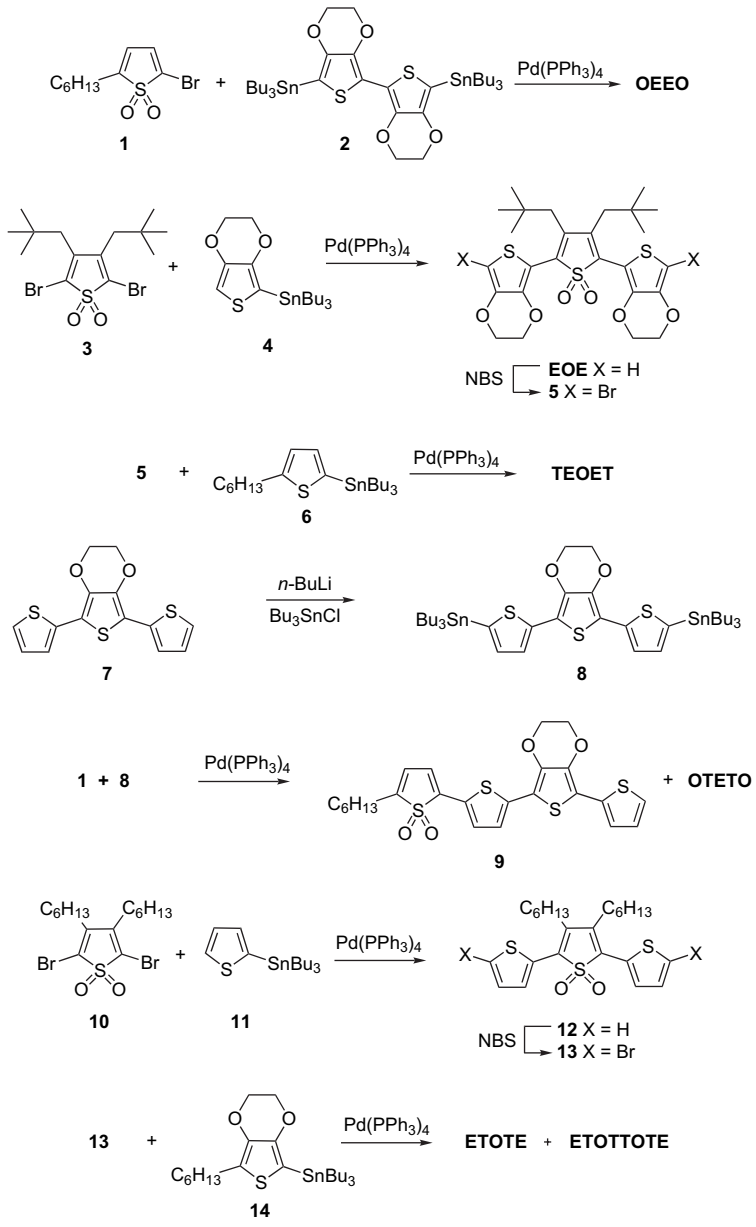

Scheme 2. Synthesis of the hybrid oligomers.

the EDOT and *S*,*S*-dioxide units allows to reduce the steric hindrance, thus favouring the planarization of the conjugated system.

2.3. Theoretical calculations

In order to analyze in more detail the influence of the relative positions of EDOT and *S*,*S*-dioxide units on the conformation and electronic properties of hybrid oligomers, theoretical calculations have been performed at the ab initio density functional level with the Gaussian 03 package. Becke's three parameter gradient corrected functional (B3LYP) with a polarized 6-31G(d) basis was used for full geometry optimization of the pentamers.

The lateral hexyl substituents were replaced by methyl groups and the median hexyl chains by butyl groups in order to limit computation time. The calculated HOMO and LUMO levels are gathered in Table 1 and the conformations adopted by the pentamers are presented in Figure 3.

Compound **TEOET** with two neopentyl chains attached at the 3 and 4 positions of the median *S*,*S*-dioxide unit presents large dihedral twist angles of 66° and 49° between the median cycle and the adjacent EDOT units due to steric interactions between the branched alkyl chains and the ethylenedioxy groups. These results agree well with the crystallographic data of the median **EOE** unit.

Replacing the two EDOT groups of **TEOET** by two unsubstituted thiophene rings and the two neopentyl groups by two linear alkyl chains as done in **ETOTE** leads to a reduction of steric interactions and thus to a decrease of the twist angles to 28° and 18°, respectively. For **OTETO** the median TET units are fully planar and the inter-ring torsion angles between this rigid terthienyl block and the two lateral

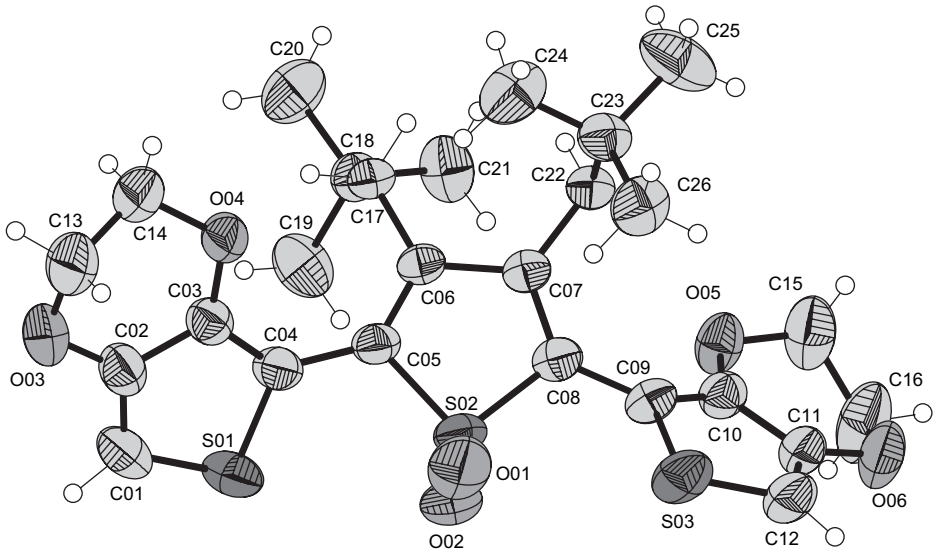

Figure 1. X-ray structure of **EOE**.

S,*S*-dioxide units are 4° and 10°, respectively. This result shows that the location of the EDOT units in the middle part of the molecule and of the bulky *S*,*S*-dioxide units in the lateral positions allows the hybrid conjugated structure to adopt an almost planar geometry. Examination of the data in Table 1 shows that **TEOET** and **ETOTE** which contain two EDOT units present higher HOMO levels than **OTETO** while, conversely, this compound which contains two terminal *S*,*S*-dioxide groups shows the lowest LUMO level.

The nearly planar compounds **ETOTE** and **OTETO** exhibit rather close HOMO–LUMO gap (ΔE). Compared to **ETOTE**, the wider gap calculated for **TEOET** which corresponds both to a decrease of HOMO level and an increase of LUMO level is essentially due to the torsion of the molecule by steric interactions (Fig. 3).

The values of LUMO and HOMO levels for planar systems **ETOTE** and **OEEO** can be compared to the values calculated with the same base for hybrid systems devoid of *S*,*S*-dioxide units **ETTTE** and **TEET**.[26] Comparison of the data for **ETOTE** and **ETTTE** shows that the insertion of electron-withdrawing unit in the middle of the molecule provokes a stronger decrease of the LUMO (−0.48 eV) than HOMO (−0.25 eV) levels, thus leading to a reduction of the gap. Results for **TEET** and **OEEO** show that replacement of the two lateral thiophene rings by *S*,*S*-dioxide units leads to higher decrease of the energy levels but always with a larger variation of the LUMO level (−1.06 eV for the LUMO and −0.63 eV for the HOMO). In contrast, compared to oligomers **OTTTO** and **OTTO**, the insertion of EDOT units in the middle of the conjugated chain produces a larger increase of the HOMO than the LUMO level. Thus, between **OTETO** and **OTTTO** the HOMO level increases

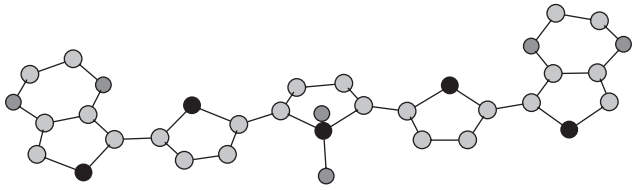

Figure 2. Structure of the conjugated backbone of **ETOTE** obtained from X-ray diffraction. The hexyl chains are not represented.

Table 1. HOMO and LUMO energy levels and gap ΔE calculated by DFT method (B3LYP/6-31G (d))

Compound	HOMO (eV)	LUMO (eV)	ΔE (eV)
TEOET	−4.87	−2.12	2.75
ETOTE	−4.65	−2.17	2.48
OTETO	−5.08	−2.69	2.39

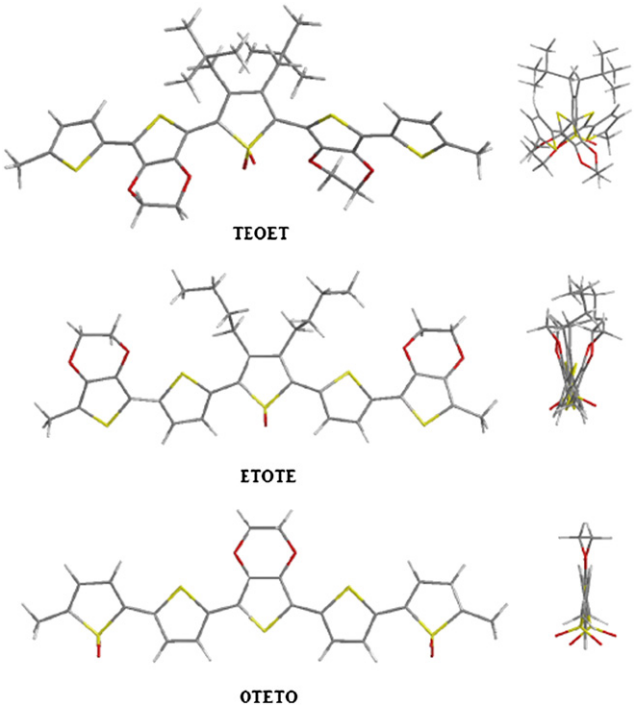

Figure 3. Optimized molecular structures of hybrid oligomers **TEOET** (top), **ETOTE** (middle) and **OTETO** (bottom).

by +0.22 eV while the LUMO raises by +0.14 eV. Between **OTTO** and **OEEO**, the HOMO and LUMO levels increase by +0.54 eV and +0.35 eV, respectively.

2.4. UV–vis spectroscopy

Table 2 lists the UV–vis absorption data of the various oligomers in dichloromethane solution. Data for other oligothiophenes containing EDOT units are also given for comparison. Oligomers with an *S*,*S*-dioxide unit in the median position present broad and structureless absorption spectra due to rotational disorder. In contrast, the spectrum of **OTETO** with EDOT moiety in the middle of the conjugated chain shows a discernible vibronic fine structure, which is better resolved in the spectrum of the tetramer **OEEO** with a bis-EDOT median unit (Fig. 4). As already observed for conjugated oligomers containing EDOT units, such spectral features are typical for planar and rigid conjugated structures in which non-bonded S···O intramolecular interactions ensure the planarization and rigidification of the molecule.[26,24,23]

Comparison of the optical spectra for **TEOET** and **ETOTE** shows that the latter compound presents a 47 nm red shift of λ_{max} and a 0.27 eV decrease of the HOMO–LUMO gap ΔE. This difference can be related to a better planarity of the molecule in agreement with X-ray data and geometry optimization. As already discussed, steric interactions between the EDOT and thiophene-*S*,*S*-dioxide units in **TEOET** result in the torsion of the conjugated chain. Conversely, replacement of neopentyl groups by hexyl groups and above all, the insertion of unsubstituted thiophene rings between the EDOT and thiophene-*S*,*S*-dioxide units leads to a decrease of the steric hindrance and thus to a planarization of the molecule.

Comparison of the UV–vis data for the hybrid EDOT-thiophene oligomers **TEET** and **ETTTE**,[26] to those for **OEEO** and **ETOTE** shows that replacement of thiophene by thiophene-*S*,*S*-dioxide produces a bathochromic shift of λ_{max} of 93 nm and 74 nm and a reduction of the gap of 0.48 eV and 0.33 eV, respectively. These results show that the association of EDOT with strong electron-acceptor building blocks leads to a significant decrease of the HOMO–LUMO gap, as already observed with other acceptor units such as cyanovinylene,[33] thienopyrazine,[34] benzothiophenedicarboximide,[35] dicyanomethylenecyclopentadithiophene[36] or benzothiadiazole[37] units.

Examination of the band edge for pentamers **ETOTE** and **OTETO** shows that the experimental gap values are not in full agreement with the results of theoretical calculations.

Table 2. Electronic absorption data for oligomers, 2×10^{-5} M in CH_2Cl_2

Compound	λ_{max} (nm)	ε (L mol^{-1} cm^{-1})	ΔE[a] (eV)
EOE	411	0.8×10^4	2.58
OEEO	517	3.0×10^4	2.21
TEOET	472	2.8×10^4	2.32
OTETO	495	3.5×10^4	2.18
ETOTE	519	3.3×10^4	2.05
ETOTTOTE	547	3.9×10^4	1.93
TEET[26]	424	2.7×10^4	2.69
ETTTE[26]	445	2.9×10^4	2.38

[a] HOMO–LUMO gap calculated from the edge of the absorption band.

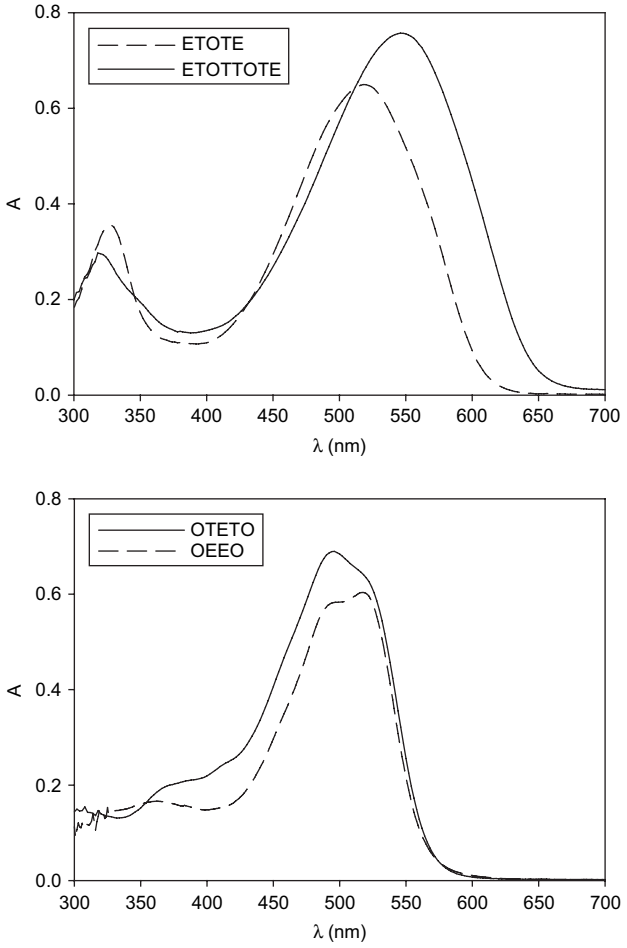

Figure 4. Electronic absorption spectra of hybrid oligomers, 2×10^{-5} M in CH_2Cl_2. Top: **ETOTE** (dotted line), **ETOTTOTE** (solid line); bottom: **OEEO** (dotted line), **OTETO** (solid line).

Indeed, although calculation indicates smaller energy gap for **OTETO**, the spectrum of **ETOTE** presents a 24 nm red shift of λ_{max} and a 0.13 eV smaller gap than **OTETO**. This result suggests that the slight torsion of compound **ETOTE** predicted by the theoretical calculation, which should produce a larger gap is counterbalanced by the non-aromatic character of the *S*,*S*-dioxide thiophene unit in the middle of the conjugated chain, which effectively allows a better electron delocalization. Another possibility could be that the structure of **ETOTE** is less twisted than predicted by calculations as suggested by the result of the crystallographic analysis of the structure of **ETOTE**. Finally, as expected the lengthening of the conjugated chain to the octamer **ETOTTOTE** leads to a large bathochromic shift of the absorption band and a decrease of the HOMO–LUMO gap concomitant with an increase of the molecular absorption coefficient.

2.5. Electrochemical properties

The electrochemical properties of the various oligomers in methylene chloride solution have been analyzed by cyclic voltammetry (CV) and the oxidation potentials of oligomers are gathered in Table 3. The CV of **EOE** presents an irreversible oxidation peak at 0.96 V and an irreversible reduction peak at −1.75 V. These values are very close to those

reported for analogous trimers in which the neopentyl groups are replaced by hexyl or dodecyl chains.[38] Application of repetitive positive potential scans leads to the emergence of a new redox system at lower potential corresponding to the electrodeposition of an electroactive polymer. As shown in Figure 5, the CV of **poly(EOE)** presents a reversible oxidation process at 0.48 V and two irreversible reduction waves at −1.55 V and −1.77 V. The reduction process leads to the degradation of the polymeric film together with an intense colouration of the solution, as already observed for the analogous polymer with dodecyl substituents.[38]

The CV of compounds **OEEO** and **OTETO** with *S*,*S*-dioxide units in the lateral positions presents irreversible oxidation and reduction peaks. Compared to **OTTO** and **OTTTO** the replacement of the inner thiophene cycles by EDOT units leads to a negative shift of both the oxidation and reduction potentials, which corresponds to an increase of the HOMO and LUMO levels due to the strong donor effect of EDOT. However, the shift of the oxidation potentials is larger than that for the reduction processes, thus leading to a reduction of the electrochemical gap ΔE_{elec}. In contrast, the reversibility of the redox processes is strongly enhanced when the thienyl-*S*,*S*-dioxide units are introduced within the conjugated chain (Fig. 6). Thus, the CV of **TEOET** presents a

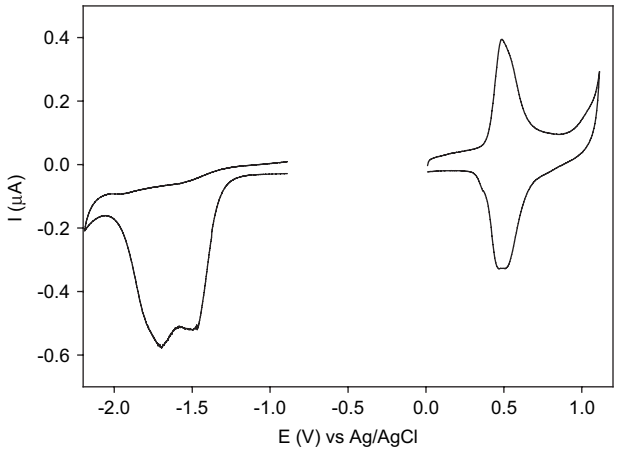

Figure 5. CV of film of **poly(EOE)** deposited on Pt disk (d=1 mm) in 0.1 M Bu_4NPF_6 in CH_3CN, reference Ag/AgCl, scan rate 50 mV s^{-1}.

Table 3. Cyclic voltammetric data[a] for oligomers

Compound	E_{ox1} (V)	E_{ox2} (V)	E_{red1} (V)	E_{red2} (V)	ΔE_{elec}[b] (eV)
EOE	0.96[c]	—	−1.75[c]	—	2.71
OEEO	0.91[c]	—	−1.43[c]	—	2.34
TEOET	0.85	—	−1.49	—	2.34
OTETO	0.89[c]	—	−1.37[c]	—	2.26
ETOTE	0.74	—	−1.37	—	2.11
ETOTTOTE	0.80	1.17	−1.24	−1.30	2.04
TEET[26]	0.48	0.92	—	—	—
ETTTE[26]	0.60	0.80	—	—	—
OTTO[28]	1.30	—	−1.18	—	2.48
OTTTO[28]	1.16	—	−1.32	—	2.48

[a] 10^{-4} M in 0.10 M Bu_4NPF_6/CH_2Cl_2, scan rate 100 mV s^{-1}, reference Ag/AgCl.
[b] $\Delta E_{elec}=E_{ox1}-E_{red1}$.
[c] Irreversible peak.

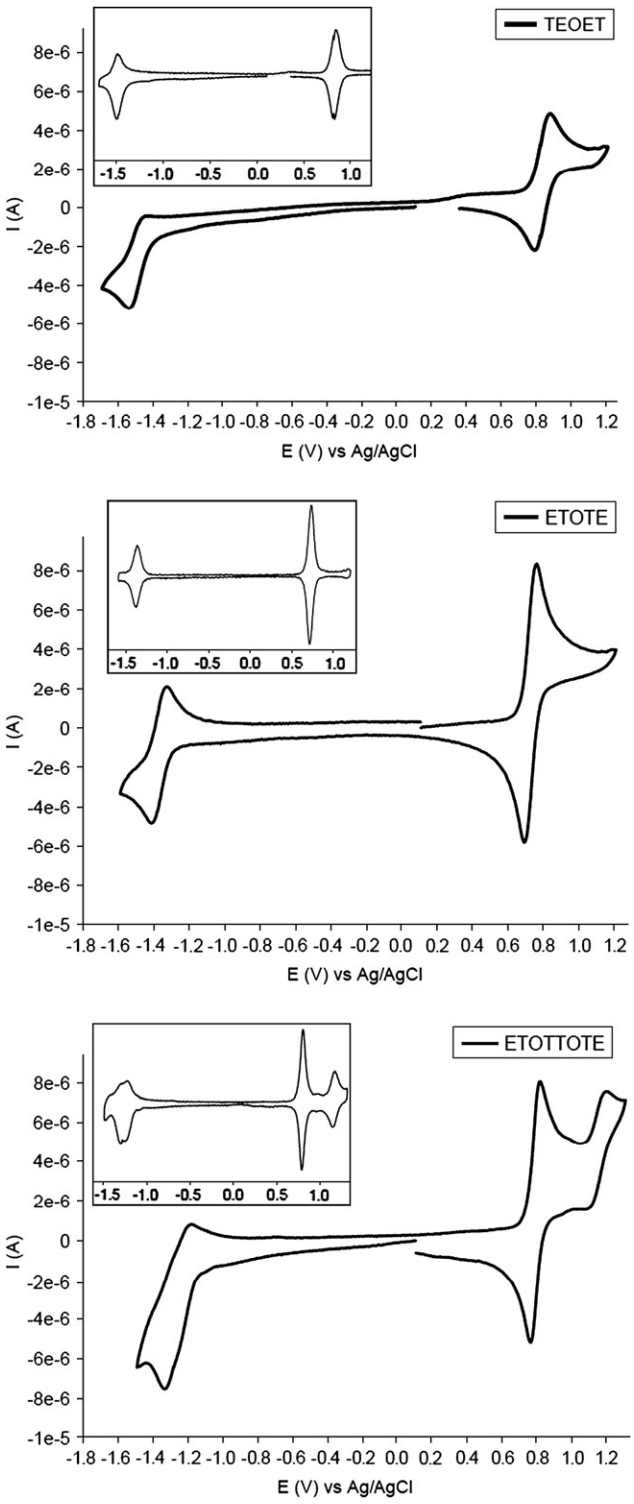

Figure 6. CV of compounds **TEOET** (top), **ETOTE** (middle) and **ETOTTOTE** (bottom) (10^{-4} mol L^{-1} in 0.1 M Bu_4NPF_6/CH_2Cl_2, scan rate 100 mV s^{-1}).

reversible monoelectronic oxidation wave and a quasi-reversible reduction peak corresponding to the formation of the cation-radical and anion-radical, respectively. The CV of **ETOTE** presents both reversible oxidation and reduction waves. For the oxidation process, the anodic–cathodic peak separation (Ep_a-Ep_c) is slightly inferior to 60 mV, thus suggesting a bi-electronic process. The deconvoluted

CV (Fig. 6 inset) confirms that oxidation leads directly to the dication state via a two-electron process while reduction leads to the radical anion through a one-electron process. Compared to **TEOET**, the shift of the EDOT units from the outer to the inner positions of the molecule provokes a strong increase of the stability of the dication state to the detriment of the cation-radical. As already observed for hybrid thiophene-EDOT oligomers[26] or oligothienylene-vinylenes incorporating EDOT units,[39] the stability of the dication results from the localization of the positive charges on the terminal EDOT units, which minimizes Coulombic repulsion. Compared to **ETTTE**, the CV of which presents two close monoelectronic oxidation processes, the formation of the dication state with a median quinoidic structure is favoured by the non-aromatic character of the central *S*,*S*-dioxide thienyl units (Scheme 3).

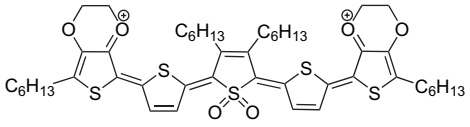

Scheme 3. Quinoidic structure for the dication **ETOTE**$^{2+}$.

Comparison of the electrochemical data for **ETOTE** and **TEOET** also reflects strong conformational differences. Thus, compared to **ETOTE**, the redox potentials of **TEOET** present both a positive shift of the oxidation peak and a negative shift of the reduction peak leading to an increase of the electrochemical gap from 2.11 eV for **ETOTE** to 2.37 eV for **TEOET**. As indicated by theoretical calculations, for **TEOET** the torsion of the conjugated chain imposed by steric interactions increases the HOMO–LUMO gap.

The similarity of the potential of the reduction peak for **OTETO** and **ETOTE** (−1.36 V vs −1.37 V) indicates that the insertion of the *S*,*S*-dioxide unit in the median position of the conjugated chain has a larger effect on the reduction potential. On the other hand, the presence of the EDOT units at the outer positions limits the positive shift of the oxidation potential resulting from the insertion of *S*,*S*-dioxide unit, and **ETOTE** presents the lowest oxidation potential of this series of hybrid oligomers.

Finally, the CV of octamer **ETOTTOTE** shows in the negative potential region a second quasi-reversible reduction peak corresponding to the formation of the dianion. It can be noticed that when using tetrahydrofuran as solvent, the CV presents two close reversible reduction waves. The lengthening of the conjugated chain and the increase of the number of electron-acceptor groups lead to the decrease of the LUMO levels and thus favours the reduction of the oligomers, as demonstrated by the positive shift of the potential peaks compared to **ETOTE**. In the positive potential region the two-electron oxidation process at 0.80 V is followed by a monoelectronic reversible peak at 1.17 V corresponding to the oxidation to trication-radical state. The first oxidation potential is higher than that for pentamer **ETOTE** indicating that the extension of the conjugated system does not compensate the electron-withdrawing effect of a second *S*,*S*-dioxide thiophene unit. These results show that the dearomatization of thiophene cycles inside the conjugated chain by the incorporation of *S*,*S*-dioxide units contributes to enhance the electron delocalization and decrease the LUMO level of the corresponding oligomers.

3. Conclusion

A new series of oligomers based on various combinations of thiophene, EDOT and thiophene-*S*,*S*-dioxide units have been synthesized. Optical, theoretical and electrochemical results have evidenced the role of the electron-releasing EDOT and electron-withdrawing *S*,*S*-dioxide moieties for modifying the HOMO and LUMO levels of the oligomers. Moreover, the results have also shown the importance of the relative positions of EDOT and *S*,*S*-dioxide units in the conjugated chain on the structure and electronic properties of the oligomers. Thus, it has been shown that the location of the self-structuring EDOT units inside the conjugated chain when the *S*,*S*-dioxide units are located at the lateral positions leads to the formation of planar conjugated systems presenting moderate band gap. By contrast, central substituted *S*,*S*-dioxide units directly coupled to EDOT moieties provoke a torsion of the conjugated chain and hence an increase of the gap. However, this torsion can be limited by separating the EDOT and *S*,*S*-dioxide moieties with unsubstituted thiophene cycles. Electrochemical data have shown that the introduction of *S*,*S*-dioxide units in the median position has a higher effect for decreasing the LUMO level while EDOT units located at the lateral positions limit the decrease of the HOMO level leading to oligomers with moderate oxidation and reduction potentials. These results show that the realization of judicious combinations of EDOT and *S*,*S*-dioxide moieties represents an efficient methodology for the fine tuning of the electronic properties of extended conjugated systems.

4. Experimental section

4.1. General

NMR spectra were recorded with a Bruker Avance DRX 500 (^{1}H, 500.13 MHz and ^{13}C, 125.75 MHz) or a Jeol GSX 270 WB (^{1}H, 270 MHz) instrument. Chemical shifts are given in parts per million relative to TMS. MALDI-TOF MS spectra were recorded on Bruker Biflex-III™ apparatus, equipped with a 337 nm N_2 laser. UV–vis spectra were recorded on a Lambda 19 instrument.

Cyclic voltammetry was performed in dichloromethane solutions purchased from SDS (HPLC grade). Tetrabutylammonium hexafluorophosphate (0.1 M or 0.2 M as supporting electrolyte) was purchased from Acros and used without purification. Solutions were deaerated by nitrogen bubbling prior to each experiment, which was run under a nitrogen atmosphere. Experiments were done in a one-compartment cell equipped with a platinum working microelectrode (∅=1 mm) and a platinum wire counter electrode. An Ag/AgCl electrode checked against the ferrocene/ferricinium couple (Fc/Fc$^+$) before and after each experiment was used as reference. Electrochemical experiments were carried out with a PAR 273 potentiostat with positive feedback compensation.

4.2. Synthetic procedure

4.2.1. 2,5-Dibromo-3,4-bis-neopentyl-(thiophene)-1,1-dioxide, 3. 2,5-Dibromo-3,4-bis-(neopentyl)-thiophene[25] (1.08 g, 26 mmol) was added to a CH_2Cl_2 solution of MCPBA (2.79 g in 30 mL). The mixture was stirred overnight at room temperature, then quenched with a solution of 10 M KOH. The organic phase was washed twice with a 10% solution of $NaHCO_3$ and then dried on $MgSO_4$. After evaporation the residue was washed with pentane to give compound **3** as a white solid (720 mg, 62% yield).

Compound **3**: mp=185 °C; ^{1}H NMR ($CDCl_3$): δ=1.01 (s, 18H), 2.52 (s, 4H). MS (EI) *m/z* 420 ($M^{+\bullet}$).

4.2.2. 3,4:3″,4″-Bis(ethylenedioxy)-3′,4′-dineopentyl-2,2′:5′,2″-terthiophene-1′,1′-dioxide, EOE. The stannic derivative of EDOT **4**[26] (1.03 g, 2.4 mmol), the brominated derivative **3** (0.40 g, 0.97 mmol) and the catalyst $Pd(PPh_3)_4$ (70 mg, 0.048 mmol) were refluxed for 3 h in dry toluene (15 mL) under inert atmosphere (N_2). After concentration, the residue was dissolved in CH_2Cl_2. The organic phase was washed twice with a saturated solution of $NaHCO_3$ and then with water. After drying on $MgSO_4$ and evaporation of solvent, the crude was purified by chromatography on silica gel (CH_2Cl_2) to give **EOE** as a yellow solid (0.39 g, 75% yield).

EOE: mp=208 °C; ^{1}H NMR ($CDCl_3$): δ=0.91 (s, 18H), 2.63 (s, 4H), 4.22 (m, 4H), 4.27 (m, 4H), 6.54 (s, 2H); ^{13}C NMR: δ=30.16, 35.24, 36.70, 64.42, 64.90, 103.38, 104.31, 129.46, 140.10, 140.36, 141.31. MS (MALDI-TOF) calcd for $C_{26}H_{32}O_6S_3$: 536.14; found: 536.27.

4.2.3. 5,5″-Dibromo-3,4:3″,4″-bis(ethylenedioxy)-3′,4′-dineopentyl-2,2′:5′,2″-terthiophene-1′,1′-dioxide, 5. To a solution of **EOE** (0.2 g, 0.37 mmol) in $CHCl_3$ (10 mL) under inert atmosphere (N_2), NBS (0.15 g, 0.84 mmol) was added in portions. The mixture was stirred during 2 h at room temperature. The solution was concentrated and the residue was dissolved in CH_2Cl_2. After washing with water, the organic phase was dried on $MgSO_4$ and then concentrated. The residue was purified by flash chromatography (CH_2Cl_2) to give **5** as a yellow solid (0.21 g, 80% yield).

Compound **5**: mp >240 °C; ^{1}H NMR ($CDCl_3$): δ=0.87 (s, 18H), 2.59 (s, 4H), 4.29 (m, 8H); ^{13}C NMR: δ=30.18, 35.36, 39.85, 64.62, 64.89, 91.83, 104.39, 128.86, 139.51, 139.76, 140.78. MS (MALDI-TOF) calcd for $C_{26}H_{30}Br_2O_6S_3$: 691.96; found: 691.91.

4.2.4. 5,5‴-Dihexyl-3′,4′,3″,4″-bis(ethylenedioxy)-2,2′:5′,2″:5″,2‴-quaterthiophene-1,1,1‴,1‴-tetraoxide, OEEO. The stannic derivative of bis-EDOT **2**[26] (440 mg, 0.40 mmol), the bromo derivative **1**[29] (260 mg, 0.93 mmol) and the catalyst $Pd(PPh_3)_4$ (28 mg, 0.024 mmol) were refluxed for 3 h in dry toluene (10 mL) under inert atmosphere (N_2). After concentration, the residue was dissolved in CH_2Cl_2. The organic phase was washed twice with a saturated solution of $NaHCO_3$ and then with water. After drying on $MgSO_4$ and evaporation of solvent, the crude was purified by chromatography on silica gel (CH_2Cl_2/PE 1:1) to give **OEEO** as an orange solid (55 mg, 20% yield).

OEEO: mp=154 °C; ^{1}H NMR ($CDCl_3$): δ=0.89 (m, 6H), 1.32 (m, 16H), 2.52 (t, ^3J=7.6 Hz, 4H), 4.41 (m, 8H), 6.45 (d, ^3J=4.8 Hz, 2H), 6.85 (d, ^3J=4.8 Hz, 2H); solubility was too low to measure its ^{13}C NMR. MS (MALDI-TOF) calcd for $C_{32}H_{38}O_8S_4$: 678.14; found: 678.03.

4.2.5. 5,5⁗-Dihexyl-3′,4′:3‴,4‴-bis(ethylenedioxy)-3″,4″-dineopentyl-2,2′:5′,2″:5″,2‴:5‴,2⁗-quinquethiophene-1″,1″-dioxide, TEOET. The Stille coupling was done according to the procedure described for **OEEO** by using 0.15 g (0.21 mmol) of **5**, 0.40 g of **6** (0.60 mmol) and 35 mg (0.03 mmol) of $Pd(PPh_3)_4$ in 10 mL of toluene. The mixture was refluxed for 8 h. After usual workups, the crude was purified by chromatography on silica gel (CH_2Cl_2) to give **TEOET** as a red solid (0.11 g, 62% yield).

TEOET: mp=130 °C; ^{1}H NMR ($CDCl_3$): δ=0.89 (s, 18H), 0.92 (t, ^3J=7.3 Hz, 6H), 1.31 (m, 16H), 2.65 (s, 4H), 2.79 (t, ^3J=7.3 Hz, 4H), 4.33 (m, 4H), 4.35 (m, 4H), 6.68 (d, ^3J=3.6 Hz, 2H), 7.10 (d, ^3J=3.6 Hz, 2H); ^{13}C NMR: δ=14.09, 22.56, 28.74, 30.10, 30.21, 31.56, 31.61, 35.35, 39.85, 64.74, 64.88, 101.11, 116.54, 123.66, 124.30, 129.00, 131.39, 136.32, 139.96, 140.21, 145.90. MS (MALDI-TOF) calcd for $C_{46}H_{60}O_6S_5$: 868.30; found: 868.15.

4.2.6. 5,5⁗-Dihexyl-3″,4″-ethylenedioxy-2,2′:5′,2″:5″,2‴:5‴,2⁗-quinquethiophene-1,1,1⁗,1⁗-tetraoxide, OTETO.

4.2.6.1. Preparation of the stannic derivative of 7. To a solution containing trimer **7**[26] (0.1 g, 0.33 mmol) dissolved in dry THF at 0 °C and under inert atmosphere (N_2), *n*-BuLi (0.45 mL of 1.6 M in hexane) was added dropwise. The mixture was stirred during 1 h at the addition temperature. Then, tributyltin chloride (2.5 equiv) was added dropwise and the mixture was stirred at the same temperature during 1/2 h before allowing to warm at room temperature. After dilution with diethyl ether, the organic phase was successively washed by a saturated solution of $NaHCO_3$, then with water. After drying on $MgSO_4$, the solvent was evaporated and the product was used without other purification in the following reactions.

4.2.6.2. Stille coupling. The Stille coupling was done by using 0.23 g (0.82 mmol) of **1**, the stannic derivative of **7** and 78 mg (0.05 mmol) of $Pd(PPh_3)_4$ in 20 mL of toluene. The mixture was refluxed for 12 h. After usual workups, the crude was purified by chromatography on silica gel (CH_2Cl_2) to give **OTETO** as a red solid (25 mg, 10% yield) and compound **9** as an orange solid (47 mg, 35% yield).

Compound **9**: mp=140 °C; ^{1}H NMR ($CDCl_3$): δ=0.88 (t, ^3J=7.0 Hz, 3H), 1.32 (m, 4H), 1.38 (m, 2H), 1.68 (m, 2H), 2.55 (t, ^3J=7.3 Hz, 2H), 4.41 (m, 4H), 6.43 (d, ^3J=4.5 Hz, 1H), 6.53 (d, ^3J=4.5 Hz, 1H), 6.97 (m, 1H), 7.04 (m, 1H), 7.18 (d, ^3J=4 Hz, 1H), 7.25 (s, shoulder $CHCl_3$ peak), 7.49 (d, ^3J=4 Hz, 1H). MS (MALDI-TOF) calcd for $C_{24}H_{24}O_4S_4$: 504.06; found: 503.94.

OTETO: mp=186 °C; ^{1}H NMR ($CDCl_3$): δ=0.89 (t, ^3J=6.9 Hz, 6H), 1.32 (m, 12H), 1.69 (m, 4H), 2.57 (t, ^3J=7.1 Hz, 4H), 4.43 (m, 4H), 6.44 (d, ^3J=4.9 Hz, 2H), 6.54 (d, ^3J=4.9 Hz, 2H), 7.21 (d, ^3J=4.0 Hz, 2H), 7.50 (d,

^3J=4.0 Hz, 2H). MS (MALDI-TOF) calcd for $C_{34}H_{38}O_6S_4$: 702.13; found: 702.05.

4.2.7. 3″,4″,5,5‴″-Tetrahexyl-3,4:3‴″,4‴″-bis(ethylenedioxy)-2,2′:5′,2″:5″,2‴:5‴,2‴″:5‴″,2‴″-quinquethiophene-1″,1″-dioxide, ETOTE. The stannic derivative of EDOT derivative **14**[24] (0.69 g, 1.07 mmol), the bromo derivative **13**[40] (0.25 g, 0.41 mmol) and the catalyst $Pd(PPh_3)_4$ (28 mg, 0.025 mmol) were refluxed for 3 h in dry toluene (10 mL) under inert atmosphere (N_2). After concentration, the residue was dissolved in CH_2Cl_2. The organic phase was washed twice with a saturated solution of $NaHCO_3$and then with water. After drying on $MgSO_4$ and evaporation of solvent, the crude was purified by chromatography on silica gel (CH_2Cl_2/petroleum ether 2:1) to give **ETOTE** as a gold green powder (0.2 g, 54% yield) and **ETOTTOTE** as a dark violet powder (20 mg, 10% yield).

ETOTE: mp=120 °C; ^{1}H NMR ($CDCl_3$): δ=0.89 (t, ^3J=6.8 Hz, 6H), 0.93 (t, ^3J=6.9 Hz, 6H), 1.30–1.39 (m, 24H), 1.61 (m, 8H), 2.66 (m, 8H), 4.25 (m, 4H), 4.32 (m, 4H), 7.18 (d, ^3J=4.1 Hz, 2H), 7.62 (d, ^3J=4.1 Hz, 2H); ^{13}C NMR: δ=14.06, 14.09, 22.57, 25.82, 27.17, 28.47, 28.78, 29.57, 30.29, 31.26, 31.51, 64.45, 65.16, 107.53, 118.11, 122.53, 126.28, 130.15, 135.51, 137.68, 138.03, 138.44. MS (MALDI-TOF) calcd for $C_{48}H_{64}O_6S_5$: 896.33; found: 896.28.

4.2.8. 3″,4″,3‴″,4‴″,5,5‴‴″-Hexahexyl-3,4:3‴‴″,4‴‴″-bis(ethylenedioxy)-2,2′:5′,2″:5″,2‴:5‴,2‴″:5‴″,2‴‴:5‴‴,2‴‴″,5‴‴″,2‴‴‴″-octathiophene-1″,1″,1‴‴″,1‴‴″-tetraoxide, ETOTTOTE. This compound was isolated as a side product in the Stille coupling for obtaining pentamer **ETOTE** (see above).

ETOTTOTE: mp=130 °C; ^{1}H NMR ($CDCl_3$): δ=0.89 (t, ^3J=6.9 Hz, 6H), 0.93 (t, ^3J=6.9 Hz, 12H), 1.30–1.38 (m, 36H), 1.52–1.64 (m, 12H), 2.64–2.71 (m, 12H), 4.25 (m, 4H), 4.34 (m, 4H), 7.19 (d, ^3J=4.0 Hz, 2H), 7.29 (d, ^3J=4.0 Hz, 2H), 7.66 (t, ^3J=3.8 Hz, 4H); ^{13}C NMR: δ=14.06, 14.09, 22.52, 22.57, 25.83, 27.13, 27.25, 28.45, 28.78, 29.57, 29.61, 30.28, 30.95, 31.25, 31.31, 31.51, 64.45, 65.16, 107.45, 118.41, 122.53, 125.27, 126.02, 128.79, 129.34, 130.90, 134.78, 137.69, 137.98, 138.37, 138.62. MS (MALDI-TOF) calcd for $C_{72}H_{94}O_8S_8$: 1342.47; found: 1342.21.

4.3. Crystallographic structures

For both crystals, crystallographic data were collected at 293 K on an STOE-IPDS diffractometer equipped with a graphite monochromator utilizing Mo Kα radiation (λ=0.71073 Å). The structures were solved by direct methods (SIR92) and refined on F^2 by full matrix least-squares techniques using SHELX-97 package. Absorption was corrected by Gaussian technique. For **EOE·CHCl$_3$**, all non-H atoms were refined anisotropically and the H atoms were included in the calculation without refinement, except for the disordered chloroform molecule where the H atom was found by Fourier difference.

For **ETOTE**, only sulfur atoms were refined anisotropically because of insufficient reflections and we prefer not to include H atoms in the calculation because of the missing C atom of the hexyl chain.

4.3.1. Crystal data for EOE·CHCl$_3$. Yellow plate ($0.62\times0.50\times0.19$ mm^3), $C_{27}H_{33}Cl_3O_6S_3$, Mr=656.06, monoclinic, space group $P2_1/n$, a=9.832(1) Å, b=20.386(2) Å, c=15.656(2) Å, β=96.30(1)°, V=3119.1(6) Å^3, Z=4, ρ_{calcd}=1.397 g cm^{-3}, μ (Mo Kα)=0.533 mm^{-1}, F(000)=1368, θ_{min}=2.00°, θ_{max}=25.91°, 30,871 reflections collected, 5873 unique (R_{int}=0.1146), restraints/parameters=4/376, R1=0.0685 and wR2=0.1975 using 4165 reflections with $I>2\sigma(I)$, R1=0.0898 and wR2=0.2140 using all data, GOF=1.065, $-0.558<\Delta\rho<1.107$ eÅ^{-3}.

4.3.2. Crystal data for ETOTE. Orange plate ($0.25\times0.19\times0.04$ mm^3), $C_{48}H_{64}O_6S_5$, Mr=897.29, triclinic, space group P-1, a=12.288(3) Å, b=14.211(3) Å, c=15.681(5) Å, α=100.95(4)°, β=107.08(3)°, γ=102.18(3)°, V=2464(1) Å^3, Z=2, ρ_{calcd}=1.209 g cm^{-3}, μ (Mo Kα)=0.280 mm^{-1}, F(000)=960, θ_{min}=1.81°, θ_{max}=26.09°, 24,210 reflections collected, 8856 unique (R_{int}=0.3338), restraints/parameters=0/258, R1=0.0897 and wR2=0.1956 using 853 reflections with $I>2\sigma(I)$, R1=0.4512 and wR2=0.3363 using all data, GOF=0.637, $-0.254<\Delta\rho<0.325$ eÅ^{-3}.

Crystallographic data (excluding structure factors) have been deposited with the Cambridge Crystallographic Data Centre under reference CCDC 648527 and 648528.

Supplementary data

Single crystal data for **EOE·CHCl$_3$** and **ETOTE**, and atomic coordinates for DFT optimizations of **ETOTE**, **TEOET** and **OTETO**. Supplementary data associated with this article can be found in the online version, at doi:10.1016/j.tet.2007.07.006.

References and notes

1. *Electronic Materials: The Oligomer Approach*; Mullen, K., Wegner, G., Eds.; Wiley-VCH: Weinheim, 1998.
2. *Handbook of Oligo and Polythiophenes*; Fichou, D., Ed.; Wiley-VCH: Weinheim, 1999.
3. Roncali, J. *Chem. Rev.* **1997**, *97*, 173–205.
4. Diederich, F.; Martin, R. E. *Angew. Chem., Int. Ed.* **1999**, *38*, 1350–1377.
5. Fichou, D. *J. Mater. Chem.* **2000**, *10*, 571–588.
6. Murphy, A. R.; Fréchet, J. M. *Chem. Rev.* **2007**, *107*, 1066–1096.
7. Dimitrakopoulos, C. D.; Malenfant, P. R. L. *Adv. Mater.* **2002**, *14*, 99–117.
8. Sun, Y. M.; Liu, Y. Q.; Zhu, D. B. *J. Mater. Chem.* **2005**, *15*, 53–65.
9. Videlot-Ackermann, C.; Ackermann, J.; Brisset, H.; Kawamura, K.; Yoshimoto, N.; Raynal, P.; ElKassmi, A.; Fages, F. *J. Am. Chem. Soc.* **2005**, *127*, 16346–16347.
10. Locklin, J.; Li, D. W.; Mannsfeld, S. C. B.; Borkent, E. J.; Meng, H.; Advincula, R.; Bao, Z. *Chem. Mater.* **2005**, *17*, 3366–3374.
11. Mitschke, U.; Bauerle, P. *J. Mater. Chem.* **2000**, *10*, 1471–1507.

12. Barbarella, G.; Melucci, M.; Sotgiu, G. *Adv. Mater.* **2005**, *17*, 1581–1593.
13. Cicoira, F.; Santato, C.; Melucci, M.; Favaretto, L.; Gazzano, M.; Muccini, M.; Barbarella, G. *Adv. Mater.* **2006**, *18*, 169–174.
14. Brabec, C. J.; Sariciftci, N. S.; Hummelen, J. C. *Adv. Funct. Mater.* **2001**, *11*, 15–26.
15. Roncali, J. *Chem. Soc. Rev.* **2005**, *34*, 483–495.
16. Segura, J. L.; Martin, N.; Guldi, D. M. *Chem. Soc. Rev.* **2005**, *34*, 31–47.
17. Roncali, J.; Frère, P.; Blanchard, P.; de Bettignies, R.; Turbiez, M.; Roquet, S.; Leriche, P.; Nicolas, Y. *Thin Solid Films* **2006**, *511–512*, 567–575.
18. Cremer, J.; Bauerle, P. *J. Mater. Chem.* **2006**, *16*, 874–884.
19. Nicolas, Y.; Blanchard, P.; Levillain, E.; Allain, M.; Mercier, N.; Roncali, J. *Org. Lett.* **2004**, *6*, 273–276.
20. Roquet, S.; Cravino, A.; Leriche, P.; Alévèque, O.; Frère, P.; Roncali, J. *J. Am. Chem. Soc.* **2006**, *128*, 3459–3466.
21. Roncali, J.; Blanchard, P.; Frère, P. *J. Mater. Chem.* **2005**, *15*, 1589–1610.
22. Groenendaal, L.; Zotti, G.; Aubert, P. H.; Waybright, S. M.; Reynolds, J. R. *Adv. Mater.* **2003**, *15*, 855–879.
23. Apperloo, J. J.; Groenendaal, L.; Verheyen, H.; Jayakannan, M.; Janssen, R. A. J.; Dkhissi, A.; Beljonne, D.; Lazzaroni, R.; Bredas, J. L. *Chem.—Eur. J.* **2002**, *8*, 2384–2396.
24. Turbiez, M.; Frère, P.; Roncali, J. *J. Org. Chem.* **2003**, *68*, 5357–5360.
25. Wasserberg, D.; Meskers, S. C. J.; Janssen, R. A. J.; Mena-Osteritz, E.; Bauerle, P. *J. Am. Chem. Soc.* **2006**, *128*, 17007–17017.
26. Turbiez, M.; Frère, P.; Allain, M.; Videlot, C.; Ackermann, J.; Roncali, J. *Chem.—Eur. J.* **2005**, *11*, 3742–3752.
27. Spencer, H. J.; Skabara, P. J.; Giles, M.; McCullough, I.; Coles, S. J.; Hursthouse, M. B. *J. Mater. Chem.* **2005**, *15*, 4783–4792.
28. Barbarella, G.; Favaretto, L.; Zambianchi, M.; Pudova, O.; Arbizzani, C.; Bongini, A.; Mastragostino, M. *Adv. Mater.* **1998**, *10*, 551–554.
29. Barbarella, G.; Favaretto, L.; Sotgiu, G.; Zambianchi, I.; Antolini, L.; Pudova, O.; Bongini, A. *J. Org. Chem.* **1998**, *63*, 5497–5506.
30. Barbarella, G.; Favaretto, L.; Sotgiu, G.; Zambianchi, M.; Bongini, A.; Arbizzani, C.; Mastragostino, M.; Anni, M.; Gigli, G.; Cingolani, R. *J. Am. Chem. Soc.* **2000**, *122*, 11971–11978.
31. Amir, E.; Rozen, S. *Angew. Chem., Int. Ed.* **2005**, *44*, 7374–7378.
32. Antolini, L.; Tedesco, E.; Barbarella, G.; Favaretto, L.; Sotgiu, G.; Zambianchi, M.; Casarini, D.; Gigli, G.; Cingolani, R. *J. Am. Chem. Soc.* **2000**, *122*, 9006–9013.
33. Thomas, C. A.; Zong, K. W.; Abboud, K. A.; Steel, P. J.; Reynolds, J. R. *J. Am. Chem. Soc.* **2004**, *126*, 16440–16450.
34. Casado, J.; Ortiz, R. P.; Delgado, M. C. R.; Hernandez, V.; Navarrete, J. T. L.; Raimundo, J. M.; Blanchard, P.; Allain, M.; Roncali, J. *J. Phys. Chem. B* **2005**, *109*, 16616–16627.
35. Sonmez, G.; Meng, H.; Wudl, F. *Chem. Mater.* **2003**, *15*, 4923–4929.
36. Berlin, A.; Zotti, G.; Zecchin, S.; Schiavon, G.; Vercelli, B.; Zanelli, A. *Chem. Mater.* **2004**, *16*, 3667–3676.
37. Raimundo, J. M.; Blanchard, P.; Brisset, H.; Akoudad, S.; Roncali, J. *Chem. Commun.* **2000**, 939–940.
38. Berlin, A.; Zotti, G.; Zecchin, S.; Schiavon, G.; Cocchi, M.; Virgili, D.; Sabatini, C. *J. Mater. Chem.* **2003**, *13*, 27–33.
39. Turbiez, M.; Frère, P.; Roncali, J. *Tetrahedron* **2005**, *61*, 3045–3053.
40. Barbarella, G.; Favaretto, L.; Sotgiu, G.; Zambianchi, M.; Arbizzani, C.; Bongini, A.; Mastragostino, M. *Chem. Mater.* **1999**, *11*, 2533–2541.